Nuclear Instruments and Methods in Physics Research A 370 (1996) 44–46

NUCLEAR INSTRUMENTS & METHODS IN PHYSICS RESEARCH Section A

ELSEVIER

Superconducting Nb–Ta–Al–AlOx–Al X-ray detectors with spatial resolution

S. Friedrich[a,*], K. Segall[a], M.C. Gaidis[a,1], D.S. Toledano[a], D.E. Prober[a], A.E. Szymkowiak[b], S.H. Moseley[b]

[a]*Yale University, Department of Applied Physics, New Haven, CT 06520-8284, USA*
[b]*NASA Goddard Space Flight Center, Greenbelt, MD 20771, USA*

Abstract

Superconducting X-ray detectors based on SIS tunnel junctions offer potential for high spectral resolution and single photon efficiency. When used in a double junction geometry, they also offer spatial resolution needed for focal plane imaging. We are developing Nb–Ta–Al–AlOx–Al detectors for space-based X-ray astronomy applications. The design employs superconductor bandgap engineering for improved charge collection and adaptability for double junction geometries. For irradiation of a single junction device with 6 keV X-rays at a single location, the detectors have an energy resolution of 87 eV at 0.27 K. Initial studies of double junction detectors show a spectral resolution of 178 eV and an inferred spatial resolution of 4 μm over an effective length of 60 μm.

1. Introduction

High resolution single photon X-ray detectors will provide an important tool for X-ray astronomy. Requirements for space-based applications are spectral resolution below 10 eV, high absorption efficiency, large effective areas (5 mm by 5 mm) and insensitivity to thermal cycling. Spatial resolution is also desired, preferably with few channels of readout, to observe spatially extended sources using focal plane imaging. Recent developments [1–3] approach the desired energy resolution, but offer spatial resolution only with a large number of separate devices.

We are developing single photon X-ray detectors based on superconductor–insulator–superconductor (SIS) tunnel junctions. Excess quasiparticles created by the absorption of a single photon are detected as an increase in the junction's subgap current, the integrated charge providing a measure of the X-ray energy. The small superconducting gap implies a theoretical energy resolution below 10 eV for X-ray energies up to 10 keV. Quasiparticle trapping can be used to minimize losses in detectors with large areas. Spatial resolution is possible by placing detectors on either side of an absorber, with each detector recording a certain fraction of the signal. The sum of the two signals is then related to the X-ray energy and their relative magnitude can be used to determine the absorption location [4]. Such a design will be attractive in applications where both high spectral and spatial resolution are needed.

2. Experiment

Tantalum and aluminum are selected as absorber and trap materials for their respective gap sizes and X-ray absorption lengths. The electrical contact to the absorber is made of niobium, whose large gap prevents the diffusion of quasiparticles into the leads. Fig. 1 shows the double junction device geometry. The two aluminum traps on either side overlap the absorber by 10 μm for fast trapping. The junction shape is chosen to minimize the magnetic field required to suppress the dc Josephson current [5]. The single junction devices have only one junction to the side of the absorber, but are otherwise identical.

Details of the geometry and the fabrication procedure have been published elsewhere [6]. The devices discussed here have absorbers 8000 Å thick with a resistance ratio $R_{300K}/R_{10K} \approx 20$ and a total area of 200 μm × 100 μm. The detector junctions have a normal state resistance of 0.6 Ω. They exhibit the expected dc Josephson current in zero magnetic field and the subgap current at low voltages follows the BCS theory down to the base temperature of our cryostat (0.25 K). At voltages above 80 μV Fiske modes cause an increase in the subgap current. For best

* Corresponding author. Tel. +1 203 432 4286, fax +1 203 432 4283, e-mail fristea@yalevm.cis.yale.edu.

[1] Present address: Downs Laboratory of Physics, California Institute of Technology, Pasadena, CA 91125, USA.

Elsevier Science B.V.
SSDI 0168-9002(95)01053-X

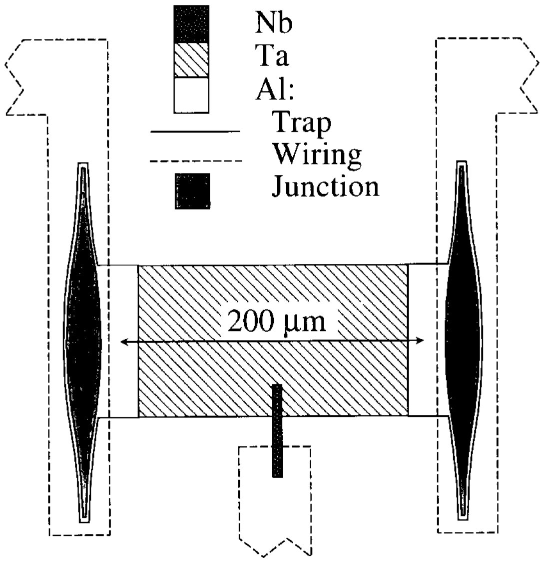

Fig. 1. Double junction detector geometry.

performance, we usually bias at the highest dynamic resistance point below the first Fiske mode. We have operated these detectors many times and do not see any changes in $I(V)$ characteristics with time or thermal cycling.

The experiments are conducted in a two stage ^{3}He cryostat. A radioactive ^{55}Fe source provides Mn X-ray lines at $E_{K\alpha} = 5.89$ keV and $E_{K\beta} = 6.49$ keV. The detector response is amplified with an A250 preamplifier with two 2SK147 FETs at its input. The input noise density was measured to be 0.4 nV/$\sqrt{\text{Hz}}$ with a $1/f$ knee at 2 kHz. For best resolution we operate the A250 as a current amplifier with a feedback resistor of 1 MΩ, although this adds 0.13 pA/$\sqrt{\text{Hz}}$ to the input noise. Current measurements are also preferred to understand quasiparticle dynamics inside the detector. We capture the entire output current waveform for each pulse with a digital oscilloscope and save the data on disk. This allows us to test the suitability of various digital filters and to eliminate multiple pulse events after the run. Charge is determined by numerical integration. We observe an increase in noise at the end of the current pulse, possibly due to a phonon mediated signal, which renders the charge measurements less accurate.

3. Results

Earlier experiments with the single junction detectors have shown varied response for different absorption locations due to different degrees of quasiparticle loss during diffusion through the absorber [7]. To reduce the spread in pulse height, we mask 90% of the absorber with a copper mask and illuminate only 20 μm at the end opposite to the junction, where the relative variations with absorption position are smallest. The best results were obtained at $T = 0.274$ K and $B = 11.25$ G at a bias voltage of 80 μV. At this bias, the thermal subgap current was 50 nA and the dynamic resistance was 9 kΩ.

The digitized current pulses were filtered with a 10 to 50 kHz first order Butterworth band pass filter. The resulting histogram is displayed in Fig. 2. The spectral resolution of the K_α line at 5.89 keV is 87 eV (FWHM). The width for injected current pulses is 47 eV and suggests an intrinsic detector resolution of 73 eV, provided that the noise sources add in quadrature. The pulser width cannot be explained by the known noise sources in the system. These sources account for less than 20 eV (FWHM), which we have verified when we replace the junction by a cold 10 kΩ resistor. This suggests that the strong non-linearity of the junction increases the electronic noise, possibly through interaction of the pulse with the Fiske mode resonance or downconversion of RF pickup. It may also not be appropriate to assume a dynamic resistance of 9 kΩ during a pulse.

The total charge is 9.1×10^6 electrons, more than the estimated 5×10^6 electrons created in the initial absorption event. Multiplication upon trapping is not effective enough to explain the magnitude of the charge by itself [7]. Backtunneling is a more likely explanation, given that the current pulse decay time is 35 μs (10 to 90%) at 0.274 K compared to a calculated tunneling time of 7 μs. This requires that the quasiparticles remain in the counterelectrode rather than diffusing out into the leads, and could indicate a degraded counterelectrode–wiring interface or anomalously slow diffusion.

The double junction experiments use two copies of the readout electronics to accommodate the two output signals from each absorption event. The device was not masked, but more than 96% of the events occur in the tantalum due to the long absorption length in the other materials. By triggering on the sum of the two signals, one can effective-

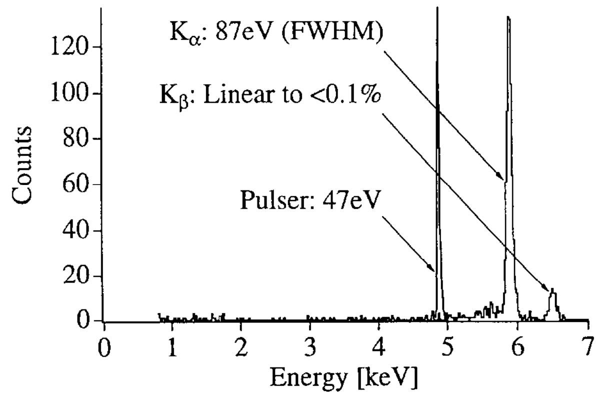

Fig. 2. X-ray spectrum of an ^{55}Fe source using a single junction detector.

ly eliminate substrate events without limiting the range of detected absorber events.

The data presented here were taken at $T = 0.32$ K in a magnetic field of $B = 13.6$ G and at a bias voltage of 70 μV. Under these conditions, both junctions have very similar characteristics ($I_{\text{bias}} = 300$ nA, $R_{\text{dyn}} = 1$ kΩ), although the two dc Josephson currents are not always suppressed equally at a given magnetic field. The output current waveforms were recorded without analog filtering, so that we can extract the physically relevant parameters from the unfiltered pulse data and then apply digital filters for best resolution. Amplitudes and risetimes of typical pulses vary between 120 nA and 2 μs (10 to 90%) for events close to one detector junction and 40 nA and 4 μs for events from the central region of the absorber. At 0.32 K decay times are roughly 19 μs, giving a combined charge of 9×10^6 electrons.

For best resolution, we use a digital 10 to 150 kHz third order Butterworth bandpass filter for the current pulses and integrate numerically to obtain the charge. Fig. 3 shows the resulting plot of the two detector responses. For large signals in one junction, the signal in the other junction is almost zero indicating good quasiparticle transmission through the absorber–trap interface. The sum of the two signals is somewhat smaller for events from the central region of the absorber due to quasiparticle losses. The degree to which the scatter plot deviates from a straight line depends on the relative time scales for quasiparticle diffusion ($\tau_{\text{diff}} = L^2_{\text{absorber}}/D$) and loss. Following Kraus' analysis [4], we can account for these losses assuming a constant ratio $\tau_{\text{diff}}/\tau_{\text{loss}}$. We estimate $\tau_{\text{diff}}/\tau_{\text{loss}} \approx 0.65$ with $\tau_{\text{diff}} \approx 1$ μs based on resistivity measurements. Assuming the loss rate does not change with absorber length, one should be able to increase the absorber size to 1.5 mm and still detect more than 10^6 electrons for X-ray absorptions anywhere along the entire length. The total energy as a function of absorption location is shown in the inset of Fig. 3. For just the central 60 μm, the spectral resolution is 178 eV. It is degraded to 198 eV if we increase the region considered to 150 μm. The electronic contribution to the noise is 57 eV. At present, we have not confined the X-ray beam to a small enough region to determine the spatial resolution directly. However, based on the energy resolution we estimate the spatial resolution to be about 4 μm [4].

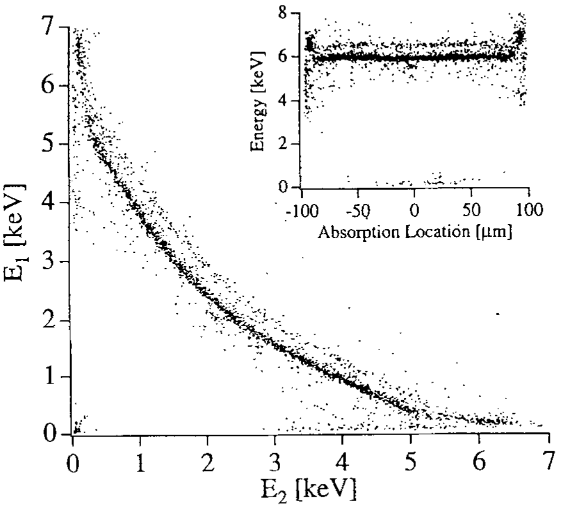

Fig. 3. Scatter plot of the two detector responses. The inset shows the sum of the two signals, corrected for loss.

A somewhat better energy resolution is obtained when the same fitting procedure is applied to the current pulse data. For the central 60 μm region, the energy resolution is 146 eV (FWHM), and over a length of 150 μm it is 174 eV. However, the equations used to normalize out losses can only be applied to the current pulses to the extent that the pulse shapes are identical so that the peak current is proportional to the charge. Future efforts will involve more precise modeling of the current pulses. We will also focus on experiments to determine the quasiparticle dynamics inside the detector and on identification of the noise sources.

In conclusion, we have demonstrated X-ray detection with all refractory superconducting SIS tunnel junction detectors using quasiparticle trapping. The spectral resolution is 87 eV (FWHM) for irradiation at a single location using a single junction detector and 178 eV with spatial resolution of 4 μm over a distance of 60 μm using double junction detectors. Better energy resolution and scaling to larger absorber areas appear possible.

References

[1] R.L. Kelley, S.H. Moseley, C.K. Stahle, A.E. Szymkowiak, M. Juda, D. McCammon and J. Zhang, J. Low Temp. Phys. 93 (1994) 225.

[2] M. Nahum and J.M. Martinis, Appl. Phys. Lett. 66 (1995) 3202.

[3] C.A. Mears, S.E. Labov and A.T. Barfknecht, J. Low Temp. Phys. 93 (1994) 561.

[4] H. Kraus, F. von Feilitzsch, J. Jochum, R.L. Mössbauer, T. Peterreins and F. Pröbst, Phys. Lett. B 231 (1989) 195;
H. Kraus, Ph.D. Thesis, Tech. University of Munich (1989).

[5] R.L. Peterson, Cryogenics 31 (1991) 132.

[6] M.C. Gaidis, S. Friedrich, D.E. Prober, A.E. Szymkowiak and S.H. Moseley, IEEE Trans. Appl. Superconductivity 3 (1993) 2961; J. Low Temp. Phys. 93 (1993) 605.

[7] M.C. Gaidis, S. Friedrich, K. Segall, D.E. Prober, A.E. Szymkowiak and S.H. Moseley, submitted to IEEE Trans. Appl. Superconductivity;
M.C. Gaidis, Ph.D. Thesis, Yale University (1994).